N62 71721

NASA TN D-1147

NASA TN D-1147

111-24
390473

TECHNICAL NOTE
D-1147

CALCULATION OF FLOW FIELDS FROM BOW-WAVE PROFILES FOR THE DOWNSTREAM REGION OF BLUNT-NOSED CIRCULAR CYLINDERS IN AXIAL HYPERSONIC FLIGHT

By Alvin Seiff and Ellis E. Whiting

Ames Research Center
Moffett Field, Calif.

NATIONAL AERONAUTICS AND SPACE ADMINISTRATION

WASHINGTON November 1961

NATIONAL AERONAUTICS AND SPACE ADMINISTRATION

TECHNICAL NOTE D-1147

CALCULATION OF FLOW FIELDS FROM BOW-WAVE PROFILES FOR THE DOWNSTREAM REGION OF BLUNT-NOSED CIRCULAR CYLINDERS IN AXIAL HYPERSONIC FLIGHT

By Alvin Seiff and Ellis E. Whiting

SUMMARY

A method by which known bow-wave profiles may be analyzed to give the flow fields around blunt-nosed cylinders in axial hypersonic flow is presented. In the method, the assumption is made that the pressure distribution curve in a transverse plane is similar to that given by blast-wave theory. Numerical analysis based on the one-dimensional energy and continuity equations then leads to distributions of all the flow variables in the cross section, for either a perfect gas or a real gas. The entire flow field need not be solved. Attention can be confined to any desired station.

The critical question is the validity of the above assumption. It is tested for the case of a hemisphere cylinder in flight at 20,000 ft/sec. The flow is analyzed for three stations along the cylindrical afterbody, and found to compare very closely with the results of an exact (inviscid) solution. The assumed form of the pressure distribution occurs at stations as close as 1.2 diameters to the body nose. However, it is suggested that the assumption may not apply this far forward in general, particularly when bodies of nonsmooth contour are considered.

INTRODUCTION

A blunt-nosed body flying at hypersonic speed creates an appreciable downstream disturbance, confined within the bow wave. The disturbance is detectable as a change in the distributions of air pressure, density, and temperature, as well as velocity. These downstream conditions have been calculated by blast-wave theory (e.g., ref. 1), and by numerical solution of the inviscid flow equations (e.g., refs. 2 and 3). Blast-wave theory gives the trends and principal features of the flow, but it does not give the details with sufficient accuracy for most purposes. The more exact theory is difficult to apply, but with the aid of modern electronic computers, it has been successfully used in a few instances.

This paper is concerned with a method of calculating the downstream flow field, given the bow-wave profile. The method is approximate in one respect; the assumption is made that the pressure distribution in a plane normal to the body axis is similar to that given by blast-wave theory. While this assumption is not directly confirmed by any previously available evidence, it appears reasonable from the following argument. The blast-wave theory gives the correct form of the equation for the bow-wave profile, requiring only an adjustment of the coefficients in the equation to fit observed wave profiles (see, e.g., ref. 4). Similarly, the trend of variation of body-surface static pressure with Mach number and drag coefficient are correctly given by the theory. Hence, it is reasonable to assume that the pressure profile in a transverse plane, which is, in fact, the primary concern of cylindrical blast-wave theory, is of the correct form. When this assumption is made, the numerical analysis is greatly simplified for the case of either a perfect gas or a real gas.

A
4
9
3

The method of analysis is similar to one described by Maslen and Moeckel, reference 5, but differs in some important respects. For example, the pressure distribution assumption described above is not made by Maslen and Moeckel. Also, in their case, the body-surface pressure distribution must be known, whereas in the present case it is considered to be unknown. In addition, they are concerned with the nose region of blunt-nosed bodies rather that the downstream region. It has not been demonstrated that their procedure can be directly applied in the downstream region. The requirement of the present method that the bow-wave profile be known is not unduly restrictive because there are so many experimental profiles available (shadowgraph pictures). For cases where the bow-wave profile is not available from experiments, reference may be made to correlations of bow-wave profiles, such as that given in reference 6. These correlations, while imperfect, permit a good first approximation to be made to the bow-wave profiles, which should, in turn, lead to a good first approximation of conditions in the disturbed flow field.

SYMBOLS

d cylinder diameter, ft

h enthalpy, Btu/lb

p static pressure, lb/sq ft

r radial coordinate, zero at body axis, ft

T static temperature, $^{\circ}$R

u local flow velocity relative to body, ft/sec x coordinate along body axis, zero at wave apex unless otherwise noted, ft

ρ air density, slugs/cu ft

Ψ angle between local stream direction and body axis, deg

Subscripts

A493

b at body

BW blast wave

i number of zone boundary

s at shock wave

∞ in free stream

METHOD OF ANALYSIS

The schematic sketch below shows the flow field under consideration and a typical streamline. The shock-wave coordinates are assumed to be known. The flow along the streamline downstream of the bow shock wave is

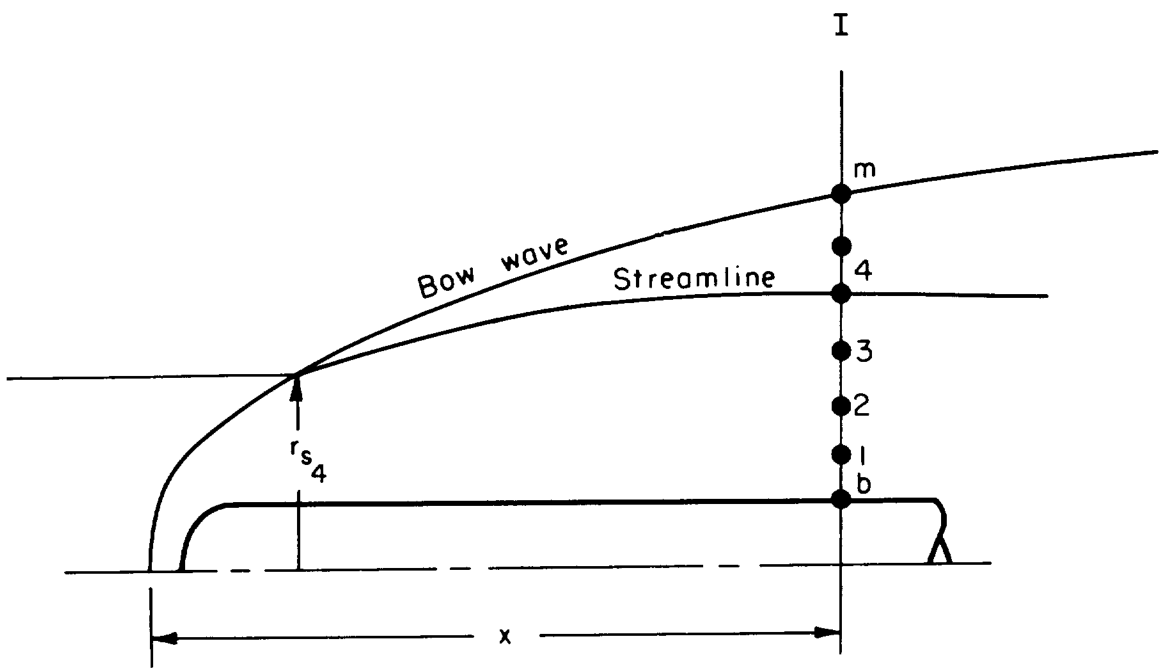

assumed to be isentropic. Since there is no mass flow across the streamline, the equation of continuity in integral form can be applied at flow station I and in the free stream to yield

$$\left(\frac{r_{s_I}}{r_b}\right)^2 = 2\int_1^{r_I/r_b} \frac{\rho}{\rho_\infty}\frac{u}{u_\infty}\frac{r}{r_b}\,d\left(\frac{r}{r_b}\right) \tag{1}$$

where r_{s_I} is the radius at which the streamline crossed the shock wave, and the integration is to be performed in the flow cross section I.

A solution is sought which will satisfy equation (1) at all points and particularly at the point m. The procedure is iterative. In the first approximation, an arbitrary but reasonable value of static pressure at the body surface is assumed. The static pressure behind the shock wave at point m is computed from the wave slope by use of the oblique shock wave relations for a real gas. The pressure distribution curve between its end points is assumed to be similar to that given by blast-wave theory, shown in figure 1, with pressure at radius r, p(r), given by

$$\frac{p(r) - p_b}{p_s - p_b} = \left[\frac{p(r) - p_b}{p_s - p_b}\right]_{BW} \tag{2}$$

The entropy at the points b, 1, 2, 3, . . ., m can be obtained from real-gas shock-wave tables (ref. 7) and air-property tables (ref. 8) provided that the location of the points r_{s_b}, r_{s_1}, r_{s_2}, . . ., r_{s_m} can be determined. The latter values are given by equation (1). Given the distributions of static pressure and entropy, one can, of course, determine any of the other state properties of the gas in the flow field.

The sequence of steps in the iteration is as follows: The solution begins at the body-surface point b. The entropy for the streamline through this point is known since $r_{s_b} = 0$. From the static pressure and the entropy, the density and enthalpy are obtained from gas tables. The velocity at the body surface (ignoring the boundary layer) is computed from the energy equation

$$h + \frac{u^2}{2} = h_\infty + \frac{u_\infty^2}{2} \tag{3}$$

The body-surface values of density and velocity are applied in the zone b-1 to obtain a first approximation to r_{s_1}. The entropy on the streamline through point 1 is calculated and used with the static pressure, gas tables, and equation (3) to obtain density and velocity at point 1. Mean values for the zone b-1 are then applied in equation (1) to improve the value of r_{s_1}.

When conditions at point 1 have converged, the process is repeated for point 2. Iterations are performed to define conditions at point 2. In this way, the solution proceeds toward point m.

In the first approximation, it will usually be found that equation (1) is not satisfied at point m. This means that for the assumed value of body-surface pressure, continuity is not satisfied. A new value of body-surface pressure is therefore chosen, guided by the direction and magnitude of the mass-flow unbalance, and the calculation repeated. Normally, no more than three repetitions of the process should be required to find a body-surface pressure which will satisfy continuity.

A
4
9
3

The number of zones needed to represent properly the air-flow profiles need not ordinarily exceed 10. The integrations through the zones can be performed graphically or by use of arithmetic mean values of density and velocity, which leads to the equation,

$$\int_{r_i}^{r_{i+1}} \rho u r \, dr = \frac{1}{2} \overline{\rho u}(r_{i+1}^2 - r_i^2) \tag{4}$$

or by assuming linear variation of the properties through the zone,

$$\int_{r_i}^{r_{i+1}} \rho u r \, dr = \left[(\rho u)_{i+1} - (\rho u)_i\right] \frac{r_{i+1}^2(2r_{i+1} - 3r_i) + r_i^3}{6(r_{i+1} - r_i)} + (\rho u)_i \frac{r_{i+1}^2 - r_i^2}{2} \tag{5}$$

Graphical integration, by allowing for curvature in the ρu profiles, is the most accurate when fairly large zone thicknesses are to be employed.

The above procedure requires about one or two man-days to produce a flow cross section by hand computation.

It should be noted that the factor $\cos \Psi$, where Ψ is the stream angle, has been omitted from equation (1), amounting to an assumption that $\cos \Psi = 1$. This should not significantly impair accuracy for downstream flow stations for the following reasons: Near the body surface, Ψ is in fact zero. At the shock wave, there is a small region where $\cos \Psi$ may take values of the order of 0.9 ($\Psi = 26^{\circ}$). Thus, the effect on the complete integral will be small. It is of some interest to note that this error could be eliminated by additional iterations after the streamline patterns are defined.

COMPARISON WITH EXACT THEORY

Solutions by the above technique should agree with more exact theory provided that the assumption represented in equation (2) is accurate. To test the agreement, comparison was made for several axial stations along a hemisphere cylinder at a flight speed of 20,000 ft/sec, and an altitude of 175,000 feet. A solution for this case was made available to the authors by the General Electric Company. It was obtained by the method of reference 2, which is a numerical solution of the complete inviscid equations for a real gas.

In order to make the comparison under similar constraints, the shock shape obtained from the General Electric solution was employed (approximately) in the present analysis. The profile of this shock wave is shown plotted on logarithmic coordinates in figure 2. The points are taken from the exact solution, and the fairing is a straight line that fits the data very well at $x/d > 0.7$. The straight line represents the shock wave assumed for the present solution and its equation is given in the figure.

The pressure distributions obtained are compared in figure 3 with those calculated by the method of reference 2 for three body stations. It can be noted that the distributions and magnitudes of the pressures are well predicted by the present method and thus assumption of equation (2) is well justified for hemisphere cylinders. The density, temperature, and velocity distributions calculated at these same three stations by the two methods are compared in figures 4, 5, and 6, respectively. Generally, the same order of agreement is obtained as in the case of the pressure distributions. The degree to which the two solutions for temperature profile possess the same undulations in profile is perhaps noteworthy. Also of interest is the high static temperature calculated to occur in the air which has passed through the strong sections of the bow wave.

Although not shown herein, the solution for a hemisphere cylinder reported in reference 3 was also compared to the distributions shown in figures 3 through 6. The conditions of speed and altitude are slightly different so that quantitative comparison is not possible, but the trends and curve shapes are entirely similar.

It was surprising to the authors to find that the assumption of equation (2) appeared to hold at the body station 1.2 diameters from the nose. It is usually said that the blast-wave theory does not have meaning in the region too close to the nose, but in the case of the hemisphere cylinder, it agrees with the shape of the pressure distribution curves rather far forward. It should probably be expected that for some other nose shapes, particularly those having discontinuities in slope, somewhat greater distances downstream would be required to develop pressure distributions of the blast-wave form.

CONCLUDING REMARKS

When the bow-wave profile associated with a blunt-nosed cylinder in
axial hypersonic flight is known, either from experiment or from correla-
tions of experimental bow waves, the method of analysis described above
can be applied to obtain a description of the enclosed flow field in the
downstream region. The results will be valid, provided that the pressure
distribution in the flow-field cross section has developed to the form
indicated by cylindrical blast-wave theory. In the case of the hemisphere
cylinder at a flight speed of 20,000 ft/sec, this condition occurs at
A stations as far forward as 1.2 diameters behind the stagnation point, and
4 the results of the analysis compare very closely with those given by more
9 exact theory. For bodies with discontinuities in slope, it can be antici-
3 pated that somewhat larger distances downstream of the nose will be
required for the pressure profiles to attain the assumed form.

Ames Research Center
National Aeronautics and Space Administration
Moffett Field, Calif., Sept. 27, 1961

REFERENCES

1. Lin, S. C.: Cylindrical Shock Waves Produced by Instantaneous Energy Release. Jour. Appl. Phys., vol. 25, no. 1, Jan. 1954, pp. 54-57.

2. Gravalos, F. G., Edelfelt, I. H., and Emmons, H. W.: The Supersonic Flow About a Blunt Body of Revolution for Gases at Chemical Equilibrium. Proc. IX International Astronautical Congress, Amsterdam, vol. 1, Aug. 25-30, 1958, pp. 312-322.

3. Feldman, Saul: A Numerical Comparison Between Exact and Approximate Theories of Hypersonic Inviscid Flow Past Slender Blunt-Nosed Bodies. AVCO-Everett Research Lab., AVCO Corp. Res. Rep. 71, June 1959.

4. Seiff, Alvin, and Whiting, Ellis E.: The Effect of the Bow Shock Wave on the Stability of Blunt-Nosed Slender Bodies. NASA TM X-377, 1960.

5. Maslen, S. H., and Moeckel, W. E.: Inviscid Hypersonic Flow Past Blunt Bodies. Jour. Aero. Sci., vol. 24, no. 9, Sept. 1957, pp. 683-693.

6. Seiff, A., and Whiting, Ellis E.: A Correlation Study of the Bow-Wave Profiles of Blunt Bodies. NASA TN D-1148, 1961.

7. Hochstim, Adolf R.: Gas Properties Behind Shocks at Hypersonic Velocities. I Normal Shocks in Air. Convair Rep. ZPh(GP)-002, Jan. 30, 1957.

8. Moeckel, W. E., and Weston, Kenneth C.: Composition and Thermodynamic Properties of Air in Chemical Equilibrium. NACA TN 4265, 1958.

A 4 9 3

A
4
9
3

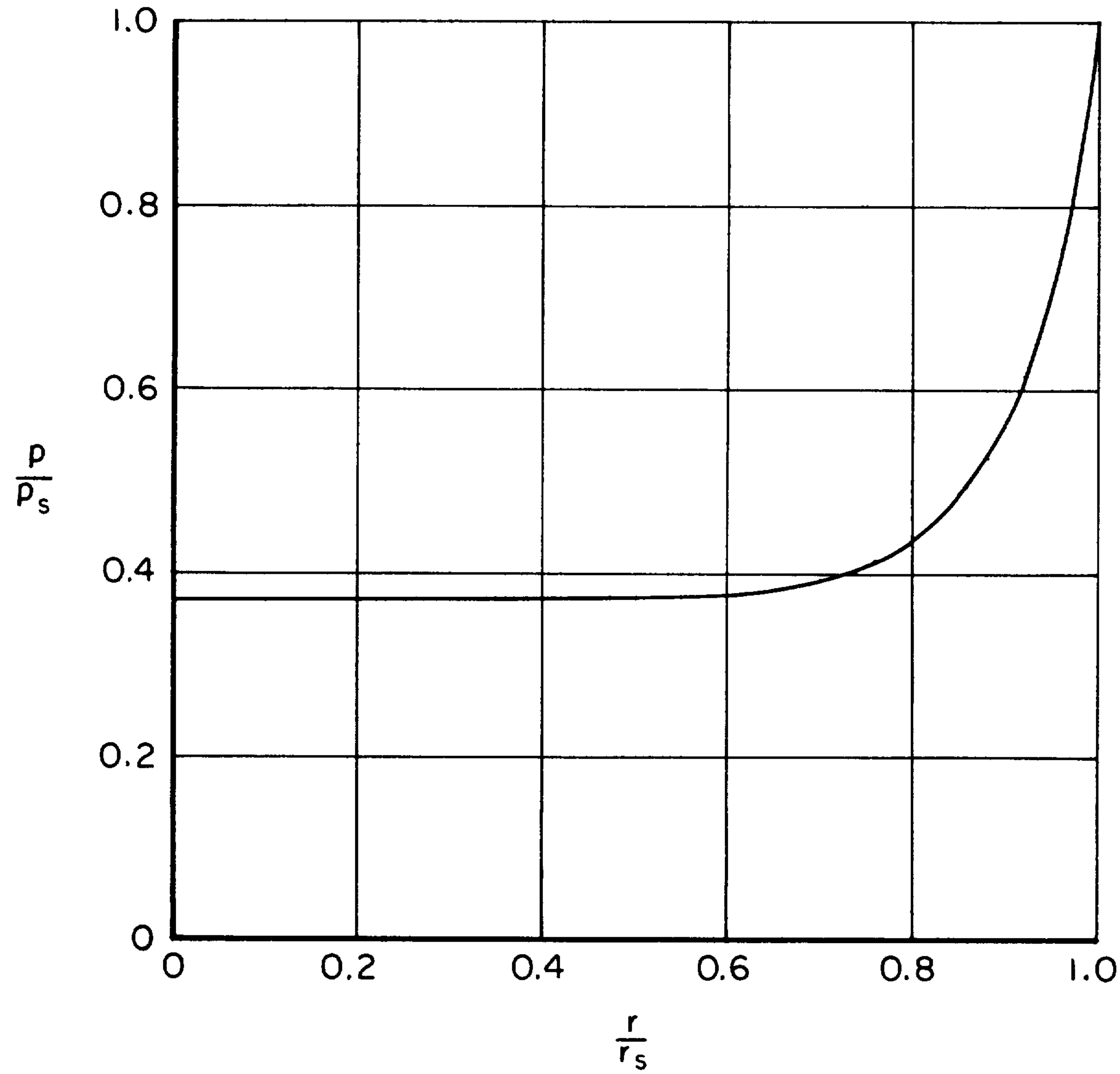

Figure 1.- Distribution of static pressure inside a cylindrical shock wave according to reference 1.

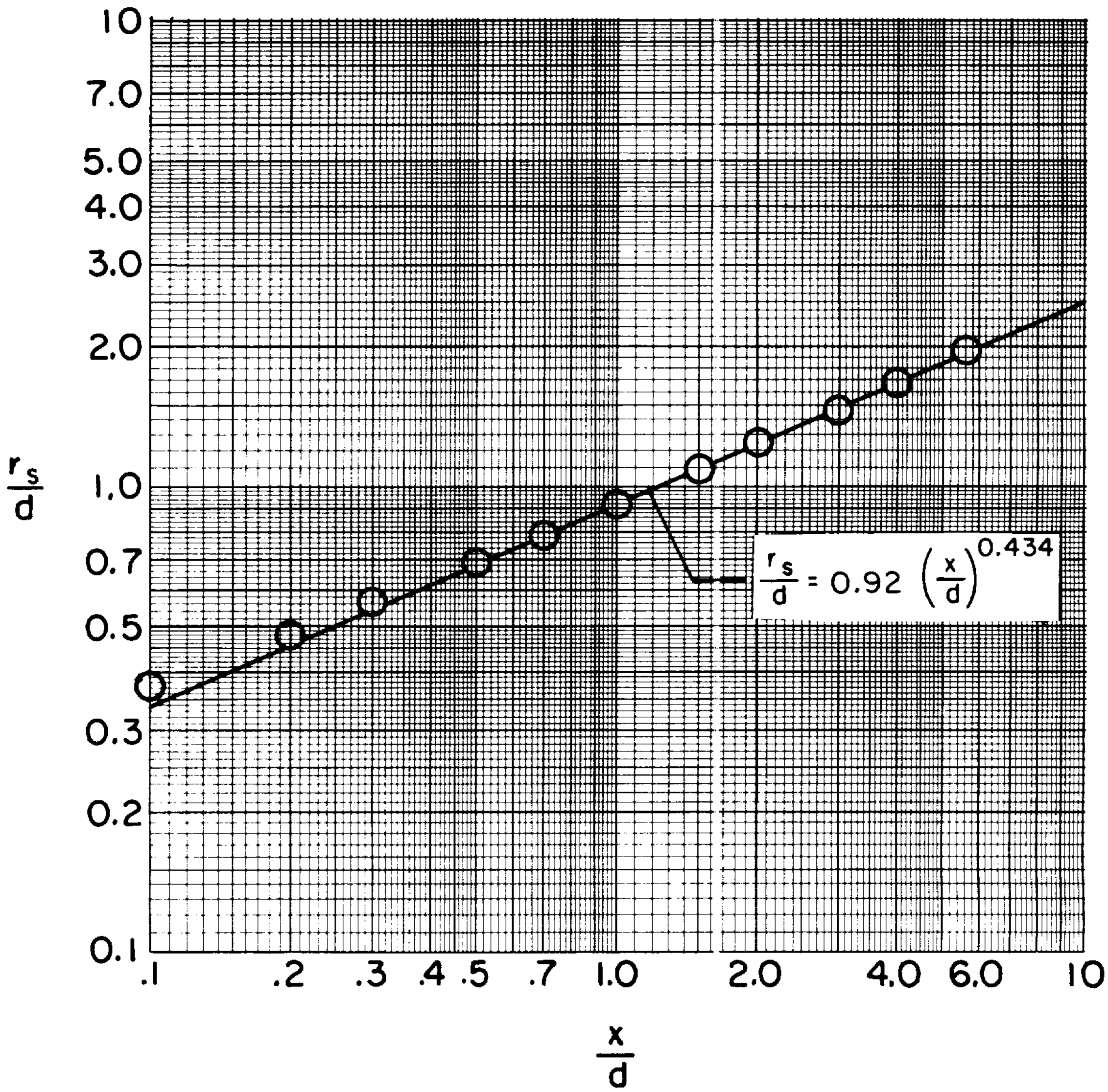

Figure 2.- Analytical approximation to shock-wave profile given by exact theory.

A
4
9
3

A 4 9 3

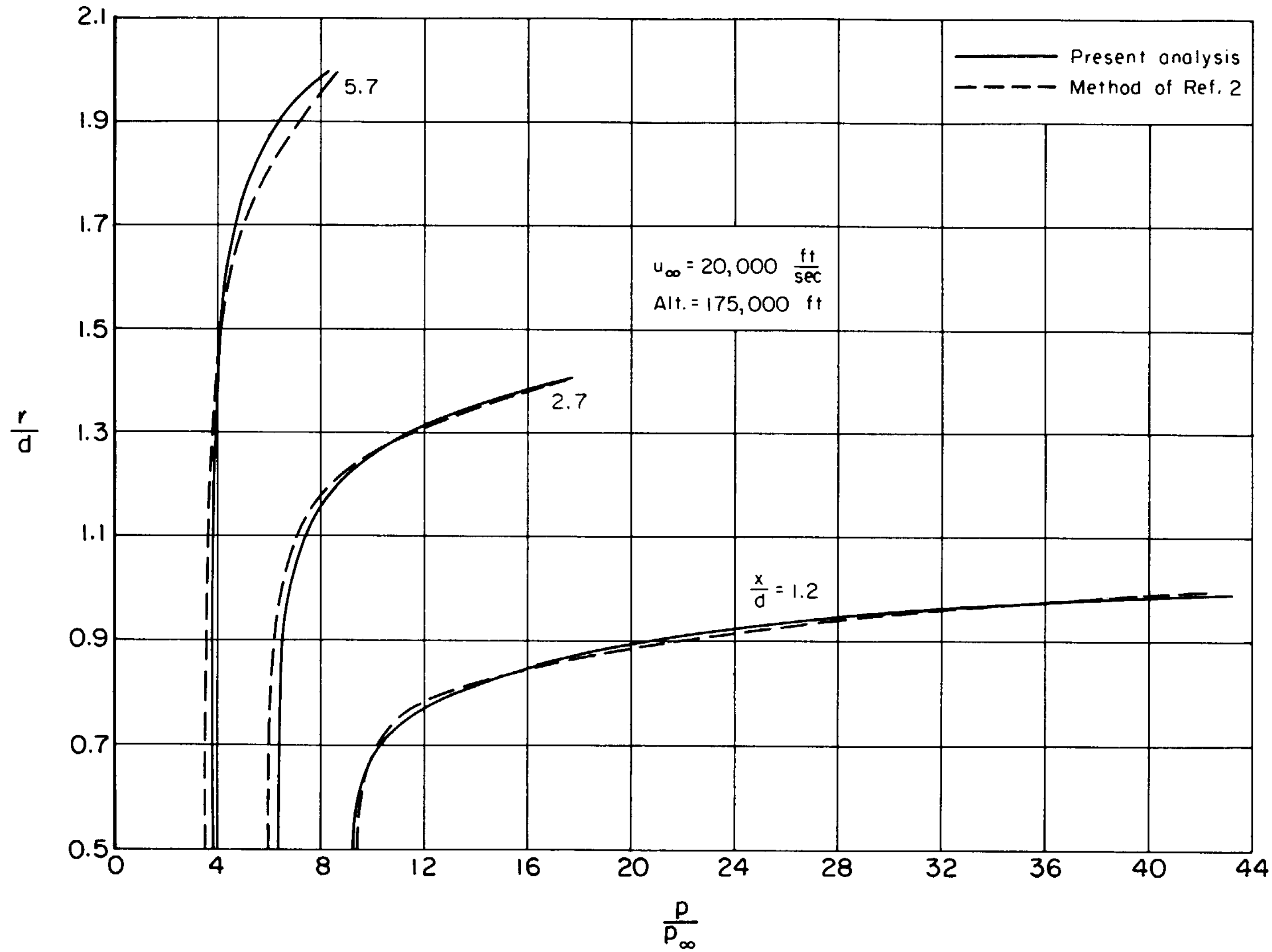

Figure 3.- Comparison of calculated static-pressure profiles for real-gas flow over a hemisphere cylinder.

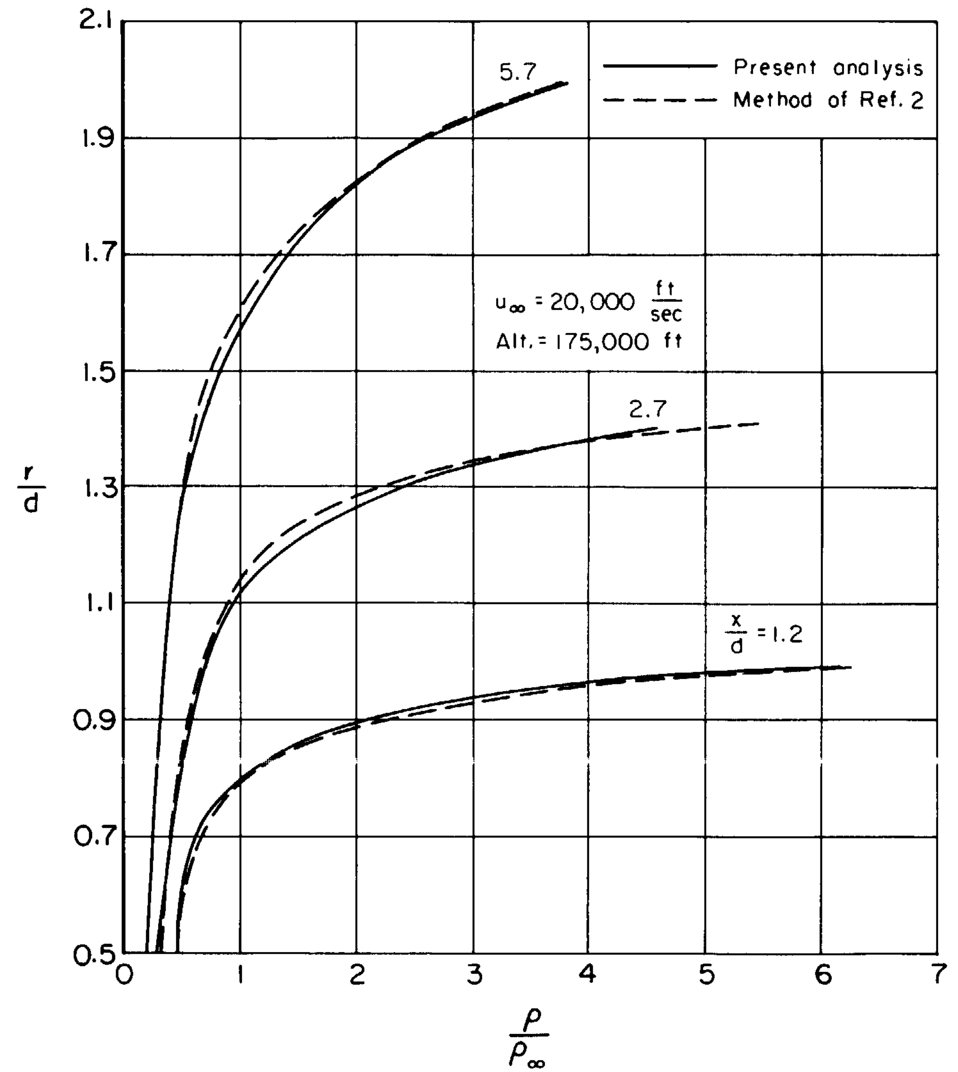

Figure 4.- Comparison of calculated density profiles for real-gas flow over a hemisphere cylinder.

A
4
9
3

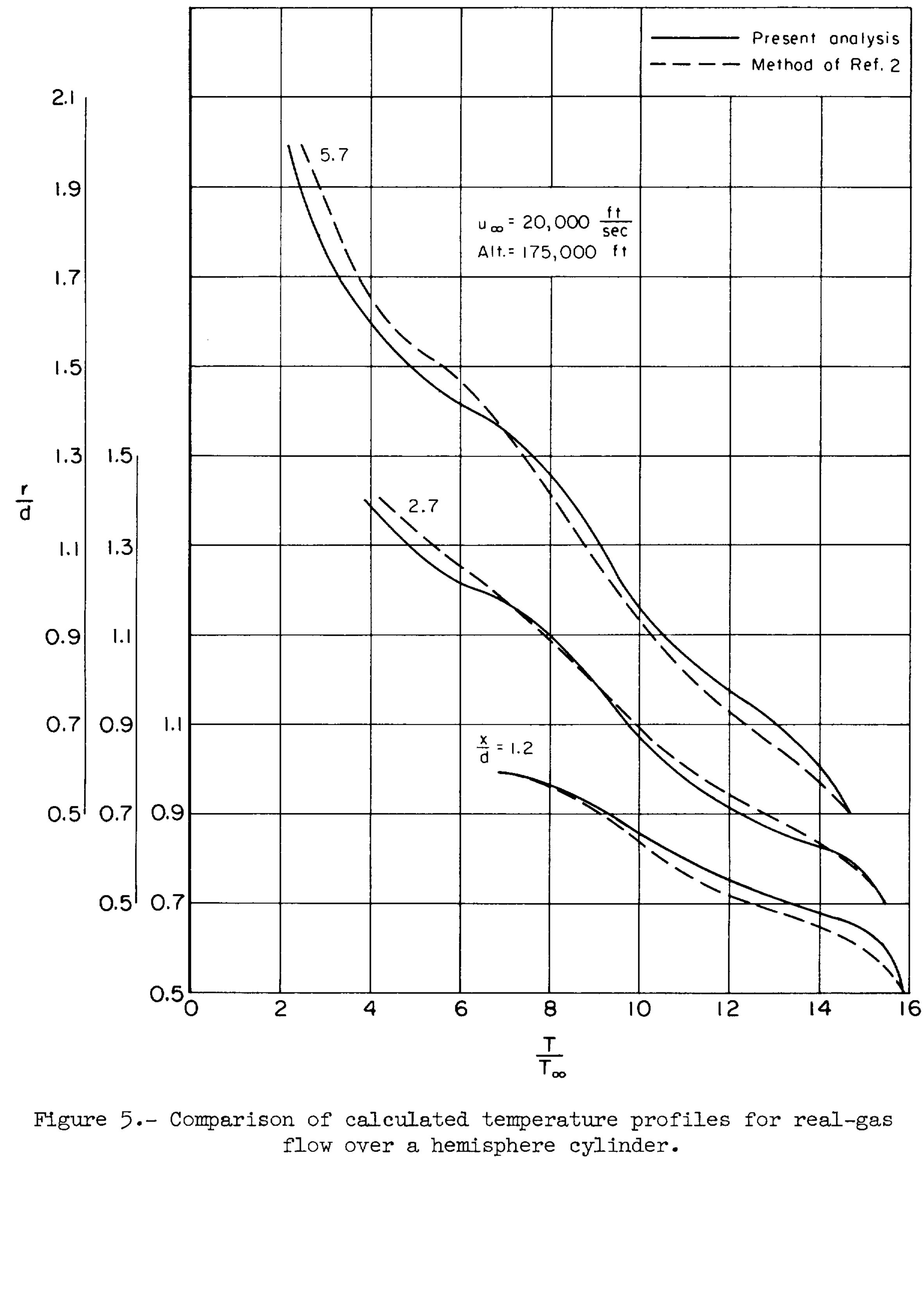

Figure 5.- Comparison of calculated temperature profiles for real-gas flow over a hemisphere cylinder.

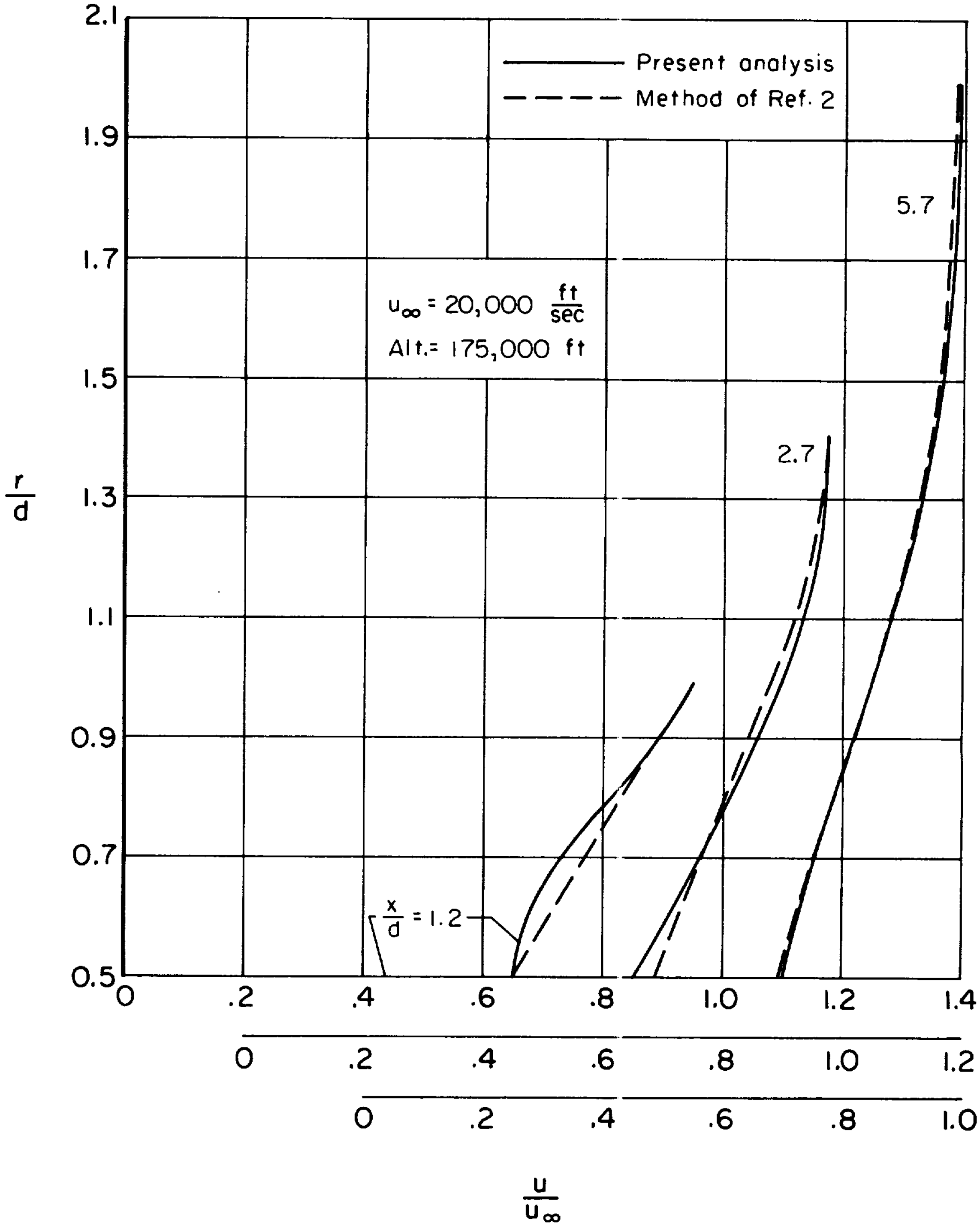

Figure 6.- Comparison of calculated velocity profiles for real-gas flow over a hemisphere cylinder.

A
4
9
3